Micromagnetic study of Ni2MnGa under applied field (invited)

Qi Pan and R. D. James

Citation: J. Appl. Phys. **87**, 4702 (2000); doi: 10.1063/1.373134
View online: http://dx.doi.org/10.1063/1.373134
View Table of Contents: http://jap.aip.org/resource/1/JAPIAU/v87/i9
Published by the AIP Publishing LLC.

Micromagnetic study of Ni_2MnGa under applied field (invited)

Qi Pan[a] and R. D. James[b]
Department of Aerospace Engineering and Mechanics, University of Minnesota, Minneapolis, Minnesota 55455

We present an experimental study of the domain and twin structure in the martensitic phase of the ferromagnetic shape memory alloy Ni_2MnGa using magnetic force microscopy. After cooling through the austenite–martensite transformation under no field, a rectangular specimen with {100} faces consistently adopted a structure of fine-scale (101) twins with surface relief, due to demagnetization effects. After cooling under a [010] field of 2 kOe, a completely different twin structure consisting of (110) parallel bands with no surface relief was observed. Under increasing fields between 2 and 8.5 kOe, the following sequence of domain structures were observed: fir tree patterns in twin bands, fir tree patterns localized at twin boundaries, single domains with thick walls (approx. 0.5 μm) coincident with twin boundaries. The domain walls exhibit unusually high contrast, and there is evidence for a wall substructure with irregularly spaced nodes. These observations are consistent with a theoretical micromagnetic study (R. D. James, Q. Pan, R. Tickle, R. Kohn, and M. Wuttig, preprint) in which approximately homogeneous rotation of magnetization occurs in alternate bands at large fields; this rotation reduces the driving force on twin boundaries before the maximum strain is achieved in some tests. © *2000 American Institute of Physics.* [S0021-8979(00)20508-2]

I. INTRODUCTION

The study of ferromagnetic shape memory, especially in the Heusler alloy Ni_2MnGa, has blossomed for both scientific and technological reasons. This alloy undergoes a reversible cubic-to-tetragonal martensitic transformation with about 3 °C hysteresis, and also is ferromagnetic. The presence of ferromagnetism offers a new handle on the martensitic transformation: by applying a field there exists the possibility either of inducing a transformation between the austenite and martensite or of rearranging the variants of martensite. Huge fields are required to induce the transformation at even a few °C above A_f, as is consistent with an appropriate form of the Clausius–Clapeyron equation, but, in the martensitic state the variants of martensite are separated by mobile twin boundaries that can be moved by moderate fields. Application of an appropriate field to a martensitic sample yields in some cases strains of around 5%, some 50 times those that are typical in giant magnetostrictive materials. Many recent investigations[1–3] have been focused on the unusually large magnetostriction. Previous experiments[1] on single crystals with polarized optical microscopy have confirmed that the large strains are produced by the field-induced rearrangement of martensitic variants.

However, a number of unexplained observations on the magnetomechanical behavior of this alloy have emerged. One of the most striking is that if a {100} rectangular crystal in the martensitic state is magnetized with a cyclic field of amplitude 10 kOe, it exhibits cyclic strains of about 0.5%–2%, depending on the shape of the specimen.[1] However, if the specimen is first ''treated'' by cooling through the austenite–martensite transformation under an appropriate stress (or field), then strains of about 5% are measured during the first subsequent cycle.[4] It has been suggested [5–7] that this pretreatment sets a particular domain structure which is favorable to the subsequent rearrangement of martensitic domains. This and other questions about domain structure motivated the present study.

The mechanism for variant rearrangement in Ni_2MnGa is partly clear. According to recent measurements,[4] the magnetocrystalline anisotropy of the single crystal martensite is about 2.5×10^6 ergs/cm^3, and the c axis is easy. (The anisotropy constant k_1 of austenite is approximately two orders of magnitude smaller than that of the martensite.) Thus, the martensite is magnetically relatively hard. An applied field in the direction of the c axis of one of the variants of martensite favors that variant, leading to large shape change.

Our observations are consistent with the following more refined picture of the mechanism. In a simple laminated twinned structure of martensite, the magnetization alternates between two values $\pm\mathbf{M}_1$ and $\pm\mathbf{M}_2$ in neighboring twin bands; the choice $\pm$ is arranged to yield (precisely) no poles on the twin boundaries; thus each band is divided by 180° domains consistent with a small overall demagnetization energy. Application of a small field (1–2 kOe) evolves this pattern to a fir tree pattern localized at the twin boundaries. Application of an intermediate field $\mathbf{H}$ (4–5 kOe) in the direction of $\mathbf{M}_2$ rotates the magnetization $\mathbf{M}_1$ only a little and therefore leads to a driving force on the twin boundaries, arising from the applied field energy $[(\mathbf{M}_2-\mathbf{M}_1)\cdot H]$. This moves twin boundaries and leads to large macroscopic strain. But the anisotropy of martensite is not sufficiently great to prevent magnetization rotation at larger fields (8–9 kOe); at such fields $\mathbf{M}_1$ rotates into $\hat{\mathbf{M}}_1$. The resulting magnetization rotation eliminates domain structure within a band, so each

[a]Also at Department of Geology and Geophysics and Institute for Rock Magnetism; Electronic mail: qipan@aem.umn.edu
[b]Electronic mail: james@aem.umn.edu

twin band (except where it meets the boundary of the specimen) coincides with a domain. At this point the twin boundaries contain substantial pole density $(\mathbf{M}_2 - \hat{\mathbf{M}}_1)\cdot\mathbf{n}$, which we see as fat boundaries with large contrast. Now the driving force on twin bands due to the applied field is reduced, the remaining difference in anisotropy energy of neighboring bands does not produce sufficient driving force to move them, and the macroscopic strain saturates.

These findings are consistent in detail with micromagnetic calculations presented elsewhere.[8] These theoretical calculations assume a simple laminated twin structure with variable volume fraction, but they allow for a fairly general subdivision of the twin bands by magnetic domains. They predict that there is homogeneous rotation within a band at the larger fields.

II. EXPERIMENTAL PROCEDURE

The specimen used for all experiments described in this article was cut from a single crystal boule with composition $Ni_{51.3}Mn_{24.0}Ga_{24.7}$, as determined by a scanning electron microscope equipped with energy dispersive spectra (EDS). The specimen dimensions were $1.2\,\text{mm}\times1.2\,\text{mm}\times8\,\text{mm}$, and the boule was oriented using Laue x-ray diffraction to obtain {100} specimen faces. The martensitic transformation temperature, determined by the magnetization versus temperature curve, is found to be 263 °K with less than 3 °K hysteresis. The Curie temperature T_c is determined by the same curve to be 358 °K. Both austenitic (below T_c) and martensitic phases are ferromagnetic in this alloy.

In order to induce the martensitic transformation, a temperature controlled specimen chamber was built. It circulates cooled nitrogen gas to maintain a temperature of around 255 °K, as measured with a thermocouple attached to the sample holder. The top face of the specimen was carefully polished to allow *in situ* observations of martensite microstructure with optical microscopy and domain structure and topography with magnetic force microscopy (MFM).

MFM observations provide very high spatial resolution approaching 20–50 nm.[9] The MFM used for the domain imaging was Digital Instruments (DI) multimode NanoScope III scanning probe microscope with an in-house built permanent magnet fixture. The magnet was sufficiently small so as to fit on the top of the piezoelectric (PZT) scanner and inside the MFM head. This allows us to apply an external in-plane field *in situ* up to 9.2 kOe at the specimen position. The NdFeB permanent magnets, yoke, and the specimen form a nearly closed magnetic circuit (gaps less than 0.1 mm). Thus flux leakage from this magnetic circuit is minimized; in all of the tests we saw no evidence (such as spurious contrast changes) that would indicate switching of the MFM tip. The typical coercive force of the hard magnetic coating CoCr tip is around 400 Oe.[10] Topographic and magnetic images were obtained with the instrument operated in tapping and lift mode using the standard MFM CoCr tips delivered by Digital Instruments. The thickness of the CoCr coatings is around 50 nm and the typical lift height is 30–50 nm.

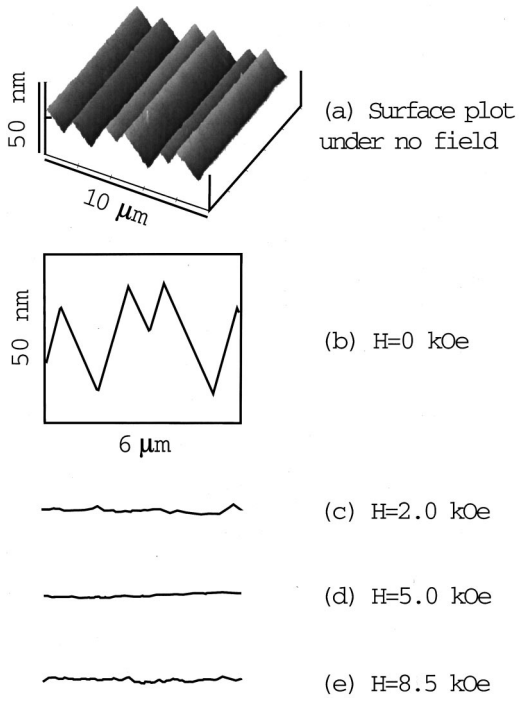

FIG. 1. A typical observation under no applied magnetic field. (a) Topographic image; (b) topographic section analysis averaged parallel to the twin boundaries; (c)–(e) typical topographic section analyses at the indicated values of the applied field.

III. OBSERVATIONS OF THE TWINS AND DOMAINS

A. Initial state with no applied field

Figure 1 shows a typical observation under no field. Here and below, all observations were done on the (001) plane, and the long axis of the specimen was parallel to [100]. Cooling through the austenite–martensite transformation under no field consistently produced twins with vertical traces, i.e., twins with normal approximately of the form $(10x)$. This twinning mode (and the other observations reported below) were always observed in our experiments, even after it was repeated many times. The mechanism of transformation was observed by optical microscopy to be the motion of a single austenite–martensite interface through the specimen. The observed twins exhibited surface relief [Figs. 1(a) and 1(b)], and the ''roof'' angle was consistent from place to place, and from test to test, and was measured to be $176.5° \pm 0.3°$. In Fig. 2(c) we show a schematic diagram of the domain structure that could produce the MFM images in Fig. 2(b). Generally the magnetic images were observed to have very high contrast, but the contrast was quite different in alternate bands. Every other band had a patchy contrast, while the remaining bands had a more homogeneous shade. This can be explained by the strong uniaxial anisotropy of the low temperature martensite phase, and the crystallography of this alloy [see below, and Fig. 2(c)]. The observations indicate that the easy axis of every other band is in-plane, while the remaining bands exhibit an easy axis perpendicular to the (100) plane.

For the reversible cubic-to-tetragonal martensitic transformation in the Ni_2MnGa system, there are three tetragonal

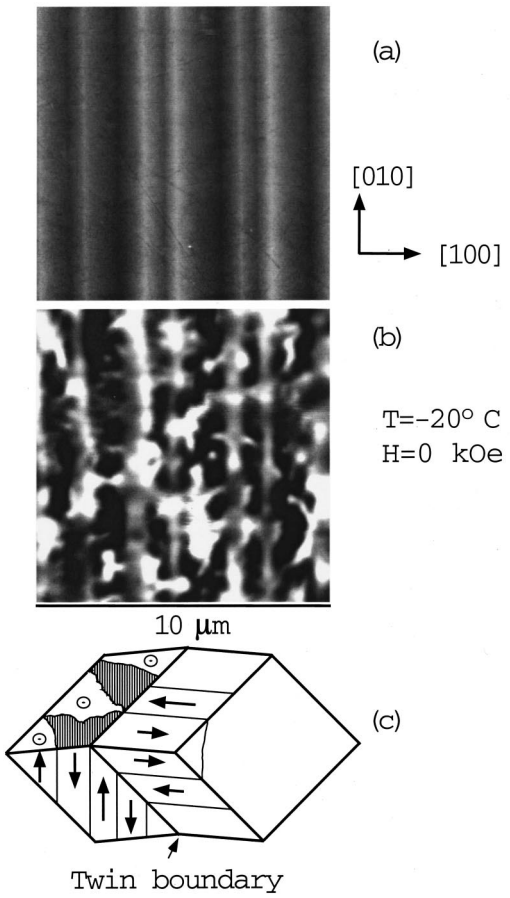

FIG. 2. A typical observation under no applied magnetic field. (a) Topographic image; (b) magnetic image showing that the magnetic contrast is quite different in alternate bands; (c) 3D schematic diagram of the twin and magnetic domain structure.

variants of martensite. These are obtained from the austenite, respectively, by linear transformations $\mathbf{U}_1=\mathrm{diag}(\eta_2,\eta_1,\eta_1)$, $\mathbf{U}_2=\mathrm{diag}(\eta_1,\eta_2,\eta_1)$, $\mathbf{U}_3=\mathrm{diag}(\eta_1,\eta_1,\eta_2)$, with $\eta_2=0.952$, $\eta_1=1.013$, which describe a shortening on the c axis and an equibiaxial expansion in the plane perpendicular to the c axis. A given pair of variants can be twinned on two different {110} planes. There are then six twin systems. The twinning is compound. If a plane is polished flat in the austenite phase, and then it is transformed to a simple twinned laminate, it will develop a roof structure of the type $\wedge\wedge\wedge$. In the present case the roof angle depends on the plane of observation and the pair of variants, but not on the twin plane. The predicted roof angles for the three pairs of variants on the (100) plane of observation are listed in Table I. These are calculated using the measured lattice parameters given above.

TABLE I. Variants and their twins in the tetragonal phase of Ni_2MnGa.

Pair of variants	Twin planes	Surface relief on (001)?	Roof angle on (001)
1 and 2	(110) and $(1\bar{1}0)$	no	180°
1 and 3	(101) and $(10\bar{1})$	yes	176.4°
2 and 3	(011) and $(01\bar{1})$	yes	176.4°

A comparison of the measured twin plane and roof angle with these calculations show excellent agreement for variants 1 and 3 twinned on either (101) or $(10\bar{1})$.

It is well known that the austenite-twinned martensite microstructure is governed by the crystallographic theory of martensite. The input to this theory is the lattice correspondence and the twinning system. Each twin system can form four different habit planes with the austenite, leading to 24 possible austenite–martensite interfaces. With no applied field, demagnetization energy should play a prominant role in determining which of these 24 are adopted, but one must also bear in mind that the experimental configuration involved the use of nitrogen gas to cool the chamber and specimen. Consequently, because of the relatively large mass from the scanner, there is expected to be a temperature gradient between the bottom (mounted on the scanner) and the top of the specimen, which could favor one or a subset of these 24 habit planes. If we consider only demagnetization energy, there is a strong preference for variant 1, because its easy axis is parallel to the long axis of the specimen. Thus, the observations are consistent with the presence of a twinned laminate of variants 1|3|1|3|1, formed during cooling by the passage of an austenite–martensite interface with low demagnetization energy.

B. Intermediate fields: 2.0–8.5 kOe

Cooling under a 2 kOe field in the direction [010] consistently produced a completely different twin system: (110) or $(1\bar{1}0)$ twins rather than (101) twins. As can be seen from Fig. 1(c), there is no surface relief, except for the random nanoscale bumps attributed to polishing. Note that from Table I, (101) twins may separate only variants 1 and 3, but

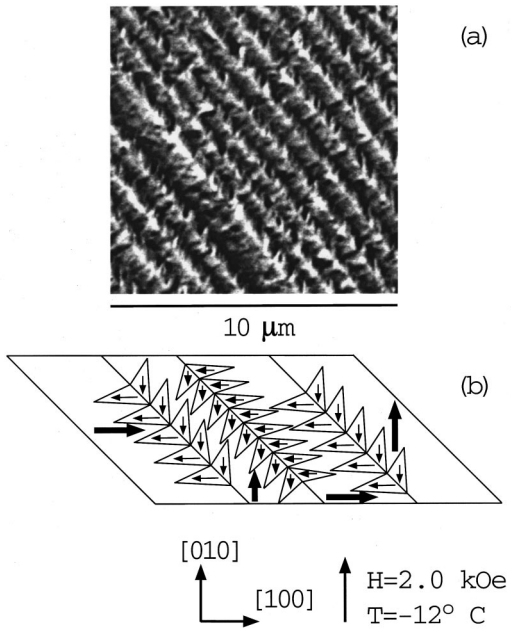

FIG. 3. (a) MFM image under 2.0 kOe applied field showing (110) twins and fir tree patterns meeting at twin boundaries; (b) 2D schematic drawing of the twin and domain structure that could produce the MFM response images (without surface relief).

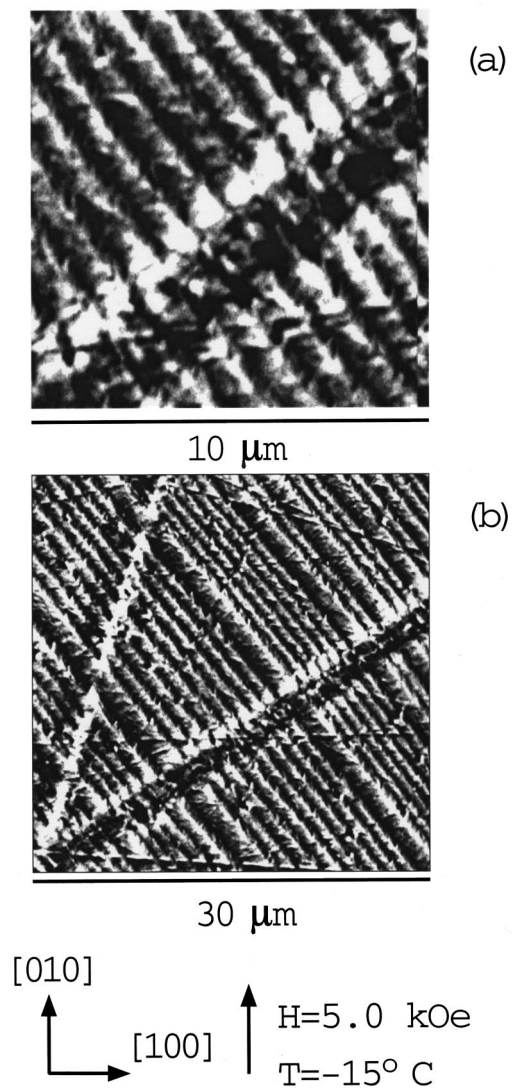

FIG. 4. (a), (b) Magnetic images under 5.0 kOe applied field. The (110) twins were observed again, but the fir tree pattern is now localized at twin boundaries. Magnetic superstructures running along the twin boundaries are apparent in (b).

neither of these has an easy axis lying in the direction [010] of the external magnetic field. The applied field favors variant 2, while demagnetization energy favors variant 1. Therefore, upon cooling under a [010] applied field it is natural to expect a mixture of variants 1 and 2 with (110) or $(1\bar{1}0)$ twinning; this was observed at all fields higher than 2.0 kOe. At 2.0 kOe the magnetic patterns along these (110) twins consists of fir tree patterns meeting at twin boundaries. The schematic drawing of the domain structure that could produce the MFM response images in Fig. 3(a) is shown in Fig. 3(b). The spike domain configuration is a common structure for the uniaxial material at an interface with poles.

We further increased the cooling field to 5.0 kOe on [010]. As expected, the (110) twins were observed again, but the fir tree pattern is now localized at twin boundaries, as shown in Fig. 4. So inside one band, from 2 to 5 kOe, the reversed spike domain shrinks and the magnetic field favors the main domain to grow. There are also some magnetic superstructures running along the twin boundaries. This is

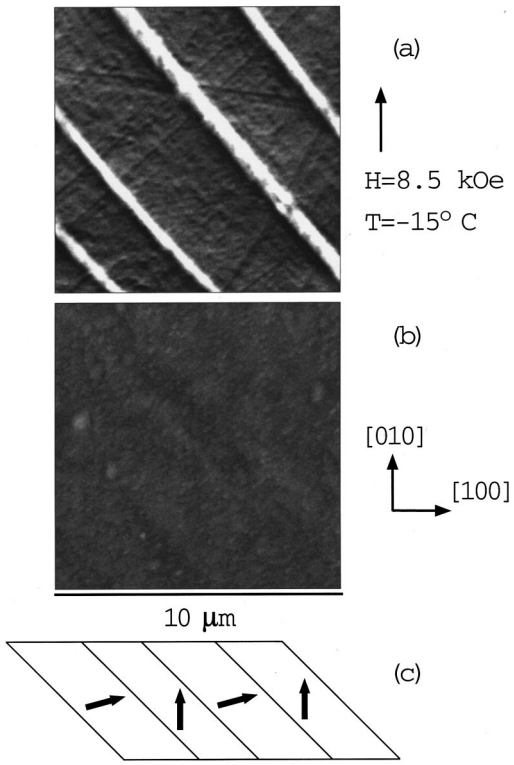

FIG. 5. (a) Magnetic and (b) topographic images under 8.5 kOe, showing no surface relief; (c) Schematic drawing of the magnetic moment distribution; note that the reversed domains have almost disappeared and the MFM patterns are very clean.

expected due to the long range magnetostatic interactions between the domains.

In the 8.5 kOe field, the reversed domains have almost disappeared. The MFM patterns are very clean and clearly show the twin magnetic domains with thick charged walls coincident with twin boundaries. The width of the twin band varies, but typically is a few microns while the domain walls are in the order of 0.5 μm. The domain walls exhibit very high contrast and a force versus distance plot (not shown) that is consistent with the presence of poles caused by magnetization rotation in alternate bands, as discussed above. There is also a wall substructure with irregularly spaced nodes, probably the traces of the reserved domains. Figure 5 gives a 10 μm square (a) magnetic and (b) topographic image under 8.5 kOe; as in all cases with applied field the twins are (110).

C. Detwinning field

Cooling through the transformation under 9.2 kOe field completely detwinned the interior of the specimen, but an unusual closure domain structure was observed at the specimen boundary (Fig. 6). At such a magnitude of the applied field, the magnetic potential energy due to the external field is so high that can induce a detwinned interior (only the variant with the easy axis along this external applied field can survives). So the whole specimen is very close to a

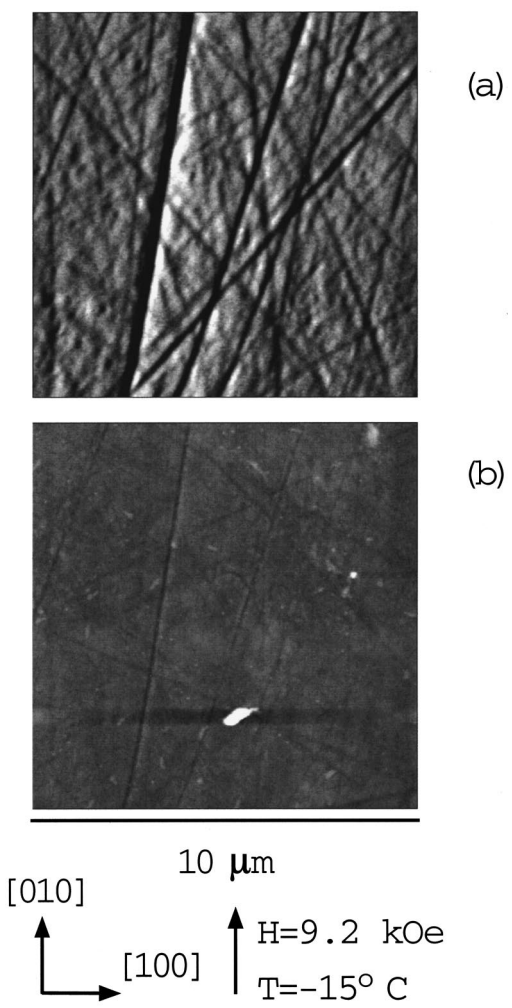

FIG. 6. (a) Magnetic and (b) topographic images under 9.2 kOe field, showing complete detwinning in the field of view. The magnetic contrast arises from the scratches.

single variant state. In the MFM images, only the constrast from scratches were observed.

On the edge of the specimen, it became more complicated. For the conventional ferromagnetic materials, the competition between the magnetostatic energy (due to the poles on the surface) and the applied field energy leads to the closure domain structure for low anisotropy material and spike reserved domain for high anisotropy one. But for this ferromagnetic shape memory material, instead of forming the closure or reserved domains on the edge of the main domain structures, thin twin structures with traces parallel to the boundary were observed on the edge of the specimen. When we scanned across these structures, we found not only strong out-of-plane magnetic response of the specimen, but also surface relief. Twin traces parallel to [100], on an (001) plane, are consistent with either of the twin planes (011) and $(01\bar{1})$, which, according to Table I can separate only variants 2 and 3, and these exhibit surface relief on (001). This pair of variants is not unexpected in such a closure twin structure, as variant 2 is present over most of the specimen, while variant 3 has no poles on the free surface [010].

ACKNOWLEDGMENTS

We wish to thank Dan Dahlberg, Bruce Moskowitz, and Rob Tickle for kindly lending us their facilities and expertise. This work was supported by ONR N00014-95-1-1145 and ONR N/N00014-99-1-0925. It also benefitted from the support of ARO DA/DAAG55-98-1-0335, AFOSR/MURI F49620-98-1-0433, and NSF DMS-9505077. This article is also a contribution 9906 of the Institute for Rock Magnetism (IRM). The IRM is supported by grants from the Keck Foundation and the NSF.

[1] R. Tickle, R. D. James, M. Wuttig, V. V. Kokorin, and T. Shield, IEEE Trans. Magn. **35**, 4301 (1999).
[2] R. D. James, R. Tickle, and M. Wutting, Mater. Sci. Eng. **273–275**, 320 (1999).
[3] K. Ulakko, J. K. Huang, C. Kantner, R. C. O'Handley, and V. V. Kokorin, Appl. Phys. Lett. **69**, 1966 (1996).
[4] R. Tickle and R. D. James, J. Magn. Magn. Mater. **195**, 627 (1999).
[5] A. DeSimone and R. D. James, preprint.
[6] R. D. James and M. Wuttig, Philos. Mag. A **77**, 1273 (1998).
[7] R. C. O'Handley, J. Appl. Phys. **83**, 3263 (1998).
[8] R. D. James, Q. Pan, R. Tickle, R. Kohn, and M. Wuttig, preprint.
[9] Y. Martin and H. K. Wickramasinghe, Appl. Phys. Lett. **50**, 1455 (1987).
[10] K. L. Babcock, V. B. Elings, J. Shi, D. D. Awschalom, and M. Dugas, Appl. Phys. Lett. **69**, 705 (1996).